

SANS and Swelling Assessment of the Structural Properties of the Thermoplastic Elastomers Santoprene™ and Sarlink™

S. V. JAECQUES,^{1,*} J. A. HELSEN,¹ and J. TEIXEIRA²

¹Department of Metallurgy and Materials Engineering, KU Leuven, De Croylaan 2, B-3001 Leuven, Belgium, and

²Laboratoire Léon Brillouin, C.E.A./C.N.R.S. Saclay, F-91191 Gif-sur-Yvette CEDEX, France;

e-mail: Siegfried.Jaecques@mtm.kuleuven.ac.be

SYNOPSIS

Two thermoplastic polyolefin elastomers, Santoprene™ 281–82 and Sarlink™ 3280, were studied by small-angle neutron scattering (SANS) and swelling. Sorption was performed in 3% (volume/volume) aqueous acetic acid (HAc) solutions at 65°C. Increase in mass and volume were followed separately. For SANS studies, swelling was also performed in D₂O solutions of HAc. Samples were subjected to mechanical fatigue, causing mainly shear stresses. A Sarlink variety with partly deuterated mineral oil was prepared to study by SANS the influence of fatigue on distribution of the oil. Absorption of the HAc solution follows Type I Fickian diffusion. Diffusion coefficients D , calculated in three ways, revealed a discrepancy between values obtained from measurements of mass or volume increase. D values were of a 10^{-13} m²/s order of magnitude. Influence of fatigue on D was not significant, although saturation liquid uptake differed markedly between fatigued and control samples. Also, remarkable differences between control Sarlink and Santoprene in saturation uptake were observed. From SANS experiments, no influence of fatigue on void size or distribution, or on distribution of mineral oil, could be observed. However, marked differences between control Sarlink and Santoprene was observed when data were interpreted in terms of fractal dimensions of phase boundaries. © 1996 John Wiley & Sons, Inc.

INTRODUCTION

Thermoplastic elastomers (TPE), more specifically, the subclass of thermoplastic polyolefins (TPO), are forming a new generic class of rubbers. They consist of a rubber phase, the terpolymer ethylene–propylene–diene (EPDM), dispersed in a polypropylene matrix (PP), and as third phase, a mineral oil is dispersed during production. The interrelation among the three phases is not well known yet. Finite element analysis (FEA) allows one to construct models that simulate fairly well the stress–strain behavior. These models are variations on a structure consisting mainly of a PP matrix that acts as the interconnecting adhesive between the rubber particles. All the deformation on stretching is absorbed by the EPDM phase to within the elastic limit of

the matrix polymer.¹ The strain recovery is dominated by the elastic modulus and yield stress of the matrix. The model, however, does not account for the role of the mineral oil.² To the best of our knowledge, no other realistic model is available. In so far as strain recovery after stretching is concerned, Santoprene behaved the best out of 10 TPEs, intercompared by Coran et al.³ From the known chemical and abrasion resistance, together with the elastic and thermoplastic properties, two commercially available products with slightly different properties were selected: Santoprene™ (Monsanto) and Sarlink™ (DSM). Both exhibited an appropriate *ensemble* of properties, fitting the orthopedic application for which we intended to use them.

As already pointed out, no model is available that accounts for the distribution of the mineral oil phase between the rubber particles in the PP matrix. Moreover, macroscopically speaking, swelling presupposes a given porosity that is also not accounted for in the published (mechanical) models. Conse-

* To whom correspondence should be addressed.

quently, it is impossible to predict what is going to happen to this distribution when the TPO is cyclically loaded for a very high number of cycles.

Having in mind applications under which the TPO will be subjected to cyclic loading in a biological environment, fatigue resistance and swelling were studied in particular. This article deals with the influence of swelling in aqueous acetic acid (HAc) and/or shearing fatigue on the small-angle neutron scattering (SANS) of Sarlink 3280 and Santoprene 218–82. The main concern was to investigate whether the distribution of the mineral oil phase and/or the void space between the PP and EPDM phases are influenced by the shearing fatigue expected in our application.

Models describing the swelling behavior of hydrogels in aqueous solutions have been published.^{4–7} However, they are not immediately applicable to the swelling behavior of our TPO in HAc solutions, because the TPO is definitely not a hydrogel. The swelling of rubber and rubber vulcanizates is a well-explored domain,^{8,9} but the organic solvents used in the published studies are always highly polar and/or aromatic solvents.^{10,11} They are used because they can dissolve the unvulcanized part of the rubber and because they rapidly cause equilibrium swelling of the vulcanizate network. At present, we are not aware of studies presenting models for the swelling of Sarlink/Santoprene-type TPO rubbers in dilute aqueous organic acid solutions, causing only a moderate swelling, as is to be expected in our application.

EXPERIMENTAL

Fatigue

The experimental setup is shown in Figure 1. Samples of $1 \times 20 \times 25 \text{ mm}^3$ were used. The machine used to apply cyclic load was a computer-monitored hydraulic compression fatigue machine (Schenck) capable of a maximum load of 7 kN. Forces were measured with a force transducer (Model Schenck PM 10 Rn) and displacements with a displacement transducer (resolution $1 \mu\text{m}$).

The sinusoidal fatigue mode was used and force was varied between 100 and 1000 N. Due to the geometry, these forces cause mainly shear stress with compressive stress only $\approx 8\%$ of shear stress. Samples can be fatigued in air or immersed in a simulated physiological solution (Hanks' solution). However, all the samples used for SANS measurements were fatigued in air.

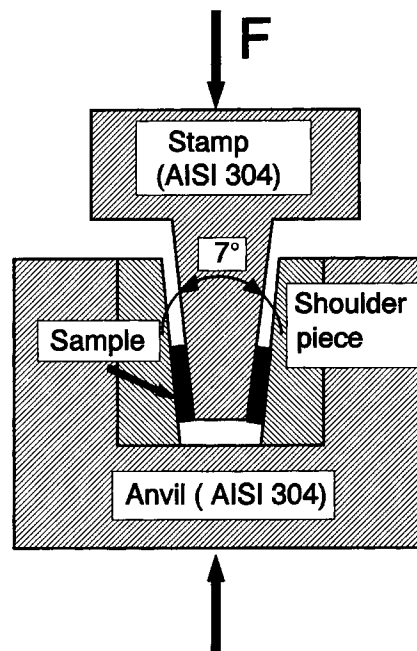


Figure 1 Cell for fatigue in air or in contact with liquids. Load angle is 3.5° . The stamp is attached to a stationary load cell while the anvil is connected to the moving part of the hydraulic cylinder of a Schenck fatigue tester.

Swelling

Liquid absorption (swelling) was determined both as relative mass change (δ_m), expressed by

$$\delta_m = \frac{m(t) - m(0)}{m(t)} \times 100\% \quad (1)$$

and as relative thickness change (δ_h), expressed by

$$\delta_h = \frac{h(t) - h(0)}{h(t)} \times 100\% \quad (2)$$

where (t) and (0) are referring, respectively, to mass or thickness at time $t = 0$ and $t = t$.

The liquid used was acetic acid (HAc) 3% (volume/volume) in H_2O . A 3% (v/v) HAc in water solution was chosen because it causes moderate and reproducible swelling of the investigated TPOs.¹² Samples were kept in the solution at a constant temperature of $(65 \pm 2)^\circ\text{C}$. Mass swelling in HAc at 65°C of five samples Santoprene 281–82 and five samples Sarlink 3280 was followed for more than 1 year (450 days). Samples were weighed at regular intervals after a standardized drying procedure to remove liquid adhering to the external surface of the samples but not yet absorbed into the bulk.

For the study of volume swelling, cylindrical samples with low thickness-to-diameter ratio were used. The diameter was 20 mm and the initial thickness ≈ 2 mm, measured for every sample with 10 μm accuracy. Samples were held between two oversized plates of sintered glass of porosity 3 (average pore diameter of 20–30 μm) of which the lower plate was resting on a solid substrate while the upper plate was in contact with the sensor of a thickness gauge with a resolution of 1 μm . Both glass plates and the lower part of the sensor were slowly immersed in the HAc solution, allowing the whole pore volume of the sintered glass to be filled with solution.

For those samples where saturation was reached, the measured data were transformed to Φ_t/Φ_s vs. $\text{time}^{1/2}$ to allow calculation of diffusion coefficients D , assuming type I Fickian diffusion. Φ_t is the volume fraction of the HAc solution in the sample at time t and Φ_s is the value of Φ at saturation. Volume fractions were calculated as [volume of HAc in the sample]/[volume of HAc in the sample + initial volume of sample]. As the samples were cylindrical, the volume V was equal to $\pi r^2 h$, with r the radius and h the height of the cylinders. The cylinders were considered as circular sheets with thickness h and radius r ; since $h/r < 0.2$, edge effects were neglected¹³ and only diffusion through the top and bottom faces of the samples was considered. Only h was assumed variable and r was assumed constant. As a matter of fact, it was observed experimentally that r does not change appreciably. In all calculations of Φ_t/Φ_s , V was replaced by h . It was assumed that the increase in thickness was caused by the penetrating solution only; in other words, the volume of 3% (v/v) HAc in water solution in the sample at time t was calculated as $h(t) - h(0)$. The equations used for the calculations of D are solutions of Fick's second law for a polymer film of thickness l in one-sided contact with water. In our case, the exposure of the polymer is two-sided. For our calculations, l will be half the sample thickness h . The sample will be saturated when both diffusion fronts meet. The two diffusion fronts do not meet at a single moment when seen on the molecular scale, as the fronts are not sharp. However, from diffusion experiments with iodine, we observed macroscopically symmetrically progressing diffusion fronts. Consequently, insofar as the macroscopic measurement of swelling is concerned, swelling progresses until the two fronts meet. Moreover, Φ_s figures in the calculations and not the time when the fronts meet. The error, if any, introduced by using half the sample thickness, will presumably be negligible.

To account for the thickness increase due to swelling, the average thickness of the samples was used. l was calculated from eq. (3):

$$l = \frac{h(0) + \frac{h(s) - h(0)}{2}}{2} \quad (3)$$

The measured data from the mass swelling experiments were converted to Φ_t/Φ_s vs. $\text{time}^{1/2}$ by dividing the appropriate masses by the appropriate densities. An equivalent l was also calculated in this way. Since the densities of 3% (v/v) HAc in water, Sarlink 3280, and Santoprene 281–82 were 1000, 950, and 980 kg m^{-3} , respectively, at the temperature of the swelling experiment, this conversion of mass to volume appears to be not really necessary, given the uncertainty on the D values.

Values for D were calculated in three ways: (a) initial slope method: in the region where $\Phi_t/\Phi_s = K \times \text{time}^{1/2}$, $D_{\text{IS}} = (K\pi^{1/2}l/2)^2$; (b) half-time method: at the time $t_{0.5}$ where $\Phi_t/\Phi_s = 0.5$ when plotted against time, $D_{0.5} = 0.04919 \times 4l^2/t_{0.5}$; and (c) nonlinear least-squares fit: the solution of Fick's second law can be written as an infinite series; if only the first two terms are considered, the solution becomes, for our experiment,

$$\frac{\Phi_t}{\Phi_s} = 1 - \frac{8}{\pi^2} \exp\left(-\frac{\pi^2 Dt}{4l^2}\right) - \frac{8}{9\pi^2} \exp\left(-\frac{9\pi^2 Dt}{4l^2}\right) \quad (4)$$

D_{NLLS} is then obtained as the result of a nonlinear least-squares fit of eq. (4) to the Φ_t/Φ_s vs. time data with D as the fit parameter. Methods (a) and (b) are well documented.^{13,14} Method (c) is based on Crank¹³ and converges most rapidly for higher values of time ($t > t_{0.5}$).

SANS

The neutron scattering data were collected at the spectrometer PAXE of the reactor Orphée at the Laboratoire Léon Brillouin (C.E.A./C.N.R.S. Saclay, France). The neutron source is from a cold neutron guide tube and monochromatization is obtained by a mechanical selector giving a wavelength width $\Delta\lambda/\lambda = 0.1$. The wavelength selected was 0.6 nm (6 Å), the sample-to-detector distance was 3 m, and the collimation was defined by two slits of diameter 10 and 7 mm, separated by a distance of 2.5 m. In this configuration, the log range of the wavevector Q covered is from -2.5 to -1.2 , corresponding to a Q range of 0.003 to 0.06 Å^{-1} . The detector

Table I Overview of the Samples Used for SANS

Sample No.	Slope of log $I - \log Q$	Description
1	-4.19	Sarlink 3280, swollen in D ₂ O + 3% HAc for 3 weeks (175 min ^{1/2}) at 65°C
2	-3.39	Sarlink 3280, swollen in H ₂ O + 3% HAc under identical conditions as sample 1
3	-4.19	Santoprene 281-82, swollen in D ₂ O + 3% HAc at 65°C
4	-3.83	Santoprene 281-82, swollen in H ₂ O + 3% HAc at 65°C
5	-3.19	Sarlink 3280 control
6	-3.90	Santoprene 281-82 control
7	-2.89	Sarlink 3280 deuterated control: during mixing of the EPDM and the PP, the mineral oil was replaced in part by a 5% (w/w) deuterated dodecane CIL 112-403 and 7% (w/w) paraffinic oil
8	-2.93	Sarlink 3280 deuterated (see sample 7), fatigued during 4 · 10 ⁶ cycles on a Schenck hydraulic fatigue tester, sinusoidally applied load, amplitude 1000-100 N at 3 Hz frequency

The raw data were processed to log $I - \log Q$ data with standard data treatment programs for normalization and incoherent background subtraction.

array consists of 64 × 64 cells of 1 × 1 cm². The incident beam was approximately in the center of the detector.

Preliminary measurements were made on control Santoprene 281-82 and fatigued Santoprene 281-82 (6.10⁶ cycles) and on deuterated Sarlink 3280, both in fatigued and fresh conditions; Table I gives an overview of the samples used in the extended experiments. As explained in the Introduction, the samples are blends of PP (approximately 25%),

EPDM (approximately 50%), mineral oil (approximately 12%), fillers, and additives. Exact details of composition are treated as industrial secrets by the manufacturers and are not available to the public. However, the blends exhibit phase inversion, as the minority component PP acts as a matrix for the EPDM. Deuterated Sarlink samples (numbers 7 and 8 in Table I) were compression-molded immediately after blending. All other samples were cut from injection-molded slabs obtained directly from the manufacturers.

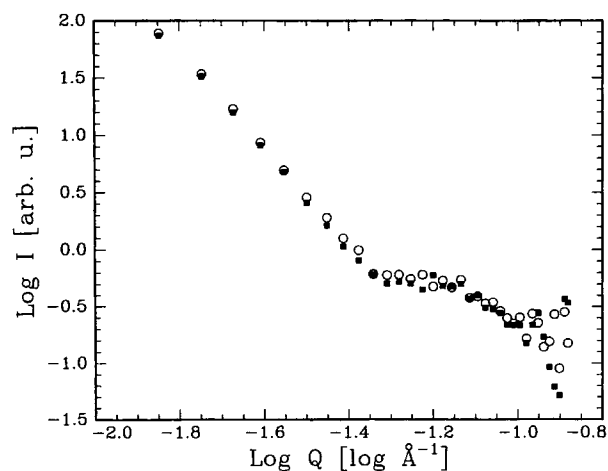


Figure 2 Results of preliminary SANS measurements on (○) control and (■) fatigued samples of Santoprene 281-82.

RESULTS

SANS

The preliminary results obtained on a control and a fatigued sample of Santoprene 281-82 are shown in Figure 2. The open symbols stand for the control sample, and the black symbols, for the one fatigued in contact with Hanks' after 6 · 10⁶ cycles. The straight-line portion of the graph has a slope quite close to -4, so Porod's law $I \sim Q^{-4}$ is applicable. I is the registered intensity of the scattered neutron beam, and Q , the scattering vector, defined as

$$Q = \frac{4\pi}{\lambda} \sin\left(\frac{\theta}{2}\right) \quad (5)$$

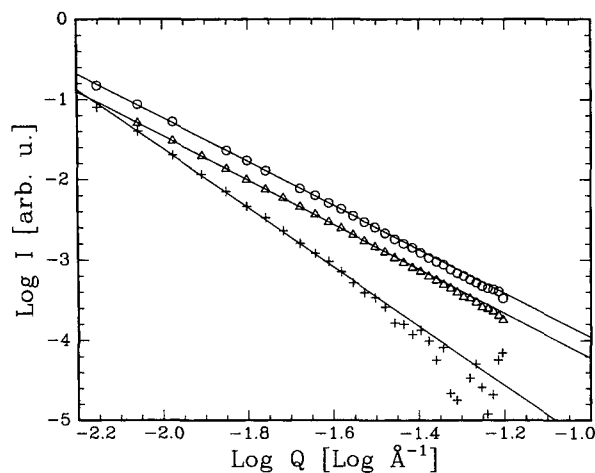


Figure 3 Results of the preliminary SANS measurements on (○) deuterated Sarlink 3280, slope -2.74 , (△) deuterated fatigued Sarlink 3280, slope -2.77 , and (+) reference Sarlink 3280, slope -3.67 .

where θ is the scattering angle, and λ , the wavelength in Å .

Figure 3 gives the results of the preliminary experiments on deuterated Sarlink 3280. A linear regression $\log I - \log Q$ in the $\log Q$ range -2.2 to -1.5 gives slopes of -2.74 , -2.77 , and -3.65 , respectively, for deuterated reference Sarlink 3280, deuterated Sarlink 3280 fatigued for $6 \cdot 10^6$ cycles, and reference Sarlink 3280 (not deuterated).

Figure 4 gives for the samples mentioned in Table I the relation $\log I - \log Q$ after removal of the incoherent background. Linear regression was made in the $\log Q$ range -2.2 to -1.5 , leading to the following observations:

1. $\log I - \log Q$ regression lines of TPO samples swollen in D_2O have the same slope (-4.19), regardless of the brand (Sarlink or Santoprene).
2. Samples 5 (Sarlink control) and 2 (Sarlink swollen in $\text{H}_2\text{O} + 3\% \text{ HAc}$) have approximately the same slope (sample 5: -3.19 , sample 2: -3.39).
3. Samples 6 and 4 also have approximately the same slope (sample 6: -3.90 ; sample 4: -3.83) and this slope is definitely greater (more negative) than with the Sarlink samples.
4. Samples 7 (deuterated Sarlink control) and 8 (deuterated Sarlink fatigued) have the same slope and this is the smallest (least negative) slope observed in all the experiments (closest to -3). These results confirm the observations made in the preliminary measurements on deuterated Sarlink 3280 (see Fig. 3).

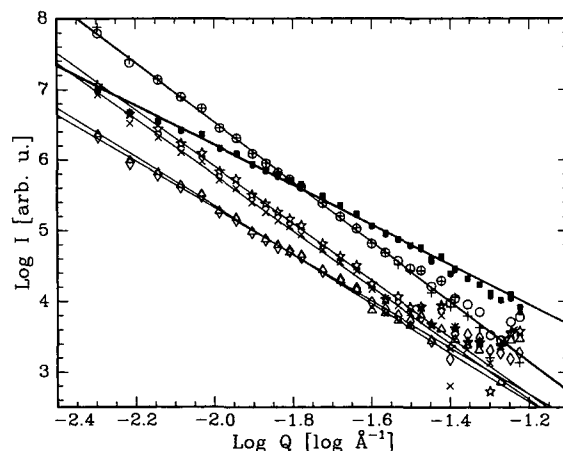


Figure 4 Comparison of SANS of a number of TPO samples. Nos. refer to sample descriptions in Table I: (○) sample 1; (△) sample 2; (+) sample 3; (×) sample 4; (◇) sample 5; (☆) sample 6; (■) sample 7; (●) sample 8.

Swelling

δ_m is plotted vs. $\text{time}^{1/2}$ in Figure 5. The error bars show 3σ on the average δ_m of five samples. This experiment was continued until saturation of the Sarlink samples. Figure 6 shows δ_n vs. $\text{time}^{1/2}$ for a control sample and a fatigued sample of Sarlink 3280. The experiment was continued until apparent saturation of the samples.

Figure 7 shows $\% \delta_n$ vs. $\text{time}^{1/2}$ for a control sample and three fatigued samples Santoprene 281-82. The experiment was continued until saturation of the control sample. The calculated diffusion coefficients for the saturated samples are listed in Table II.

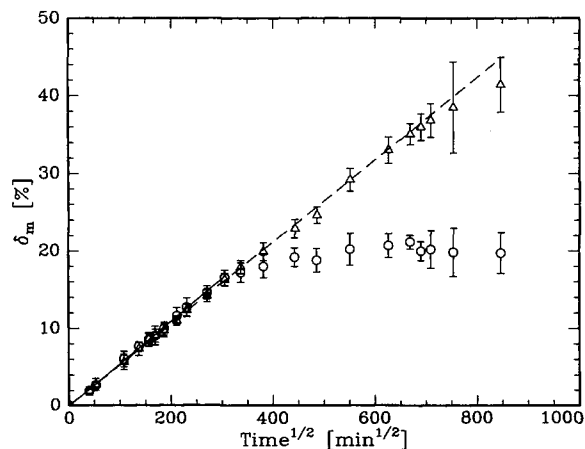


Figure 5 Mass swelling in $\text{HAc } 3\% \text{ (v/v)}$ of (△) Santoprene 281-82 and (○) Sarlink 3280: average values of δ_m vs. $(\text{time})^{1/2}$. Error bars are 3σ on the average values.

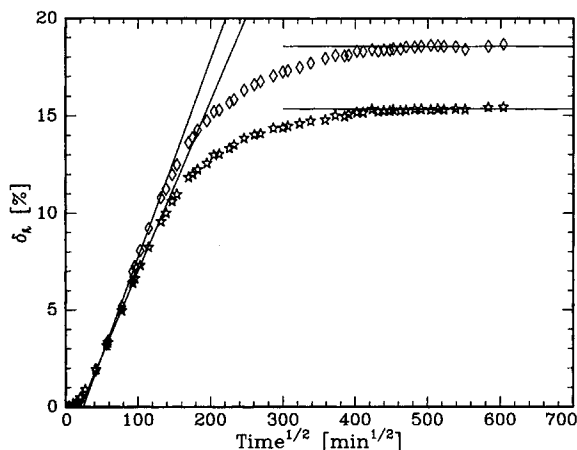


Figure 6 Volume swelling of (\diamond) fatigued and (\star) control Sarlink 3280.

DISCUSSION

Swelling

For the volume swelling of fatigued and control Santoprene 281-82, the part at low time^{1/2} values was discussed elsewhere¹²; the conclusion was that the fatigue had led to an increase in porosity of the TPO. This conclusion is now supported by the higher saturation values of δ_h for the fatigued samples.

The mass swelling experiment on control samples reveals quite a different saturation value for Sarlink 3280 (ca. 20% δ_m) and Santoprene 281-82, still swelling (more than 40% δ_m) after more than 1 year of immersion. This points, for Santoprene 281-82 as compared to Sarlink 3280, to higher porosity or higher pore volume and higher driving force for swelling. The results of SANS measurements support this conclusion: Compared to Sarlink 3280, the slope of $\log I - \log Q$ for Santoprene 281-82 points to sharper phase boundaries and/or larger voids between the EPDM and PP phase constituting the TPO Santoprene 281-82. This interpretation of $\log I - \log Q$ curves in terms of voids and phase boundaries was discussed by Teixeira.^{15,16} For Sarlink, there is a good accordance between the results of the mass swelling and the volume swelling in the sense that saturation is reached over the time^{1/2} range 350-500 min^{1/2} in both experiments. For Santoprene, volume swelling reaches saturation at significantly smaller time^{1/2} values than does mass swelling. This is difficult to explain, but it might be related to the small but apparently not negligible force (1 ± 0.1 N) exerted by the sensors of the micrometer gauges onto the surface of the samples.

The time lag, observed in the volume swelling experiments (Figs. 6 and 7) and apparently not in mass swelling, cannot yet be explained. This time lag also complicates the analysis of the volume swelling data.

For mass swelling of Sarlink, the diffusion coefficients calculated by the three different methods are identical to two significant figures. The diffusion coefficients calculated from volume swelling for a control sample of Sarlink 3280 are three to four times larger than the diffusion coefficient calculated from mass swelling. Also, the diffusion coefficient calculated from increase in thickness tends to increase with increasing values of time, while the diffusion coefficient calculated from increase in mass does remain constant. These facts might indicate that increase in mass and increase in thickness of Sarlink samples, immersed in a 3% (v/v) HAc solution, do not scale as one should expect. At the moment, we have no reasonable explanation for this phenomenon.

The difference between the diffusion coefficients of fatigued and control Sarlink samples is probably not significant ($p > 0.1$). This could be expected assuming the hypothesis that only microcracks are initiated by fatigue,¹² not modifying the intrinsic properties of the polymer, as is clear from the data for Sarlink. Due to lack of experimental evidence, the question remains open as to whether this is also the case for Santoprene.

The calculated diffusion coefficients are low when compared to literature values for the diffusion coefficient of pure water vapor at 25°C into polyethylene at 25°C (230×10^{-13} m²/s)^{17,18} and into polypropylene (240×10^{-13} m²/s).^{17,18} However, these are values for water vapor, not liquid water with 3% (v/v) HAc,

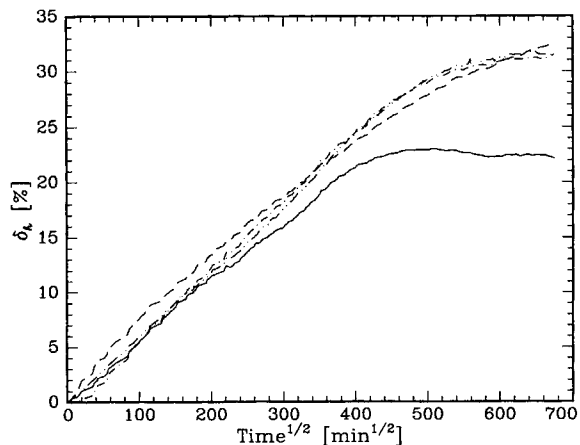


Figure 7 Volume swelling of (—) control and [(· · ·)] 3.0E4 cycles; (---) 3.0E5 cycles; (---) 4.8E6 cycles fatigued samples Santoprene 281-82.

Table II Calculated Diffusion Coefficients for Saturated Samples

Method	Sample	D_{IS} (m ² /s)	$D_{0.5}$ (m ² /s)	D_{NLLS} (m ² /s)
Mass swelling	Sarlink 3280 control	1.2×10^{-13}	1.2×10^{-13}	1.2×10^{-13}
Volume swelling	Sarlink 3280 control	5.6×10^{-13}	4.1×10^{-13}	3.2×10^{-13}
	Sarlink 3280 fatigued	4.4×10^{-13}	3.0×10^{-13}	2.5×10^{-13}
	Santoprene 281-82 control	1.5×10^{-13}	1.4×10^{-13}	1.3×10^{-13}

and Sarlink 3280 cannot be compared straightforwardly with a pure polymer like polypropylene. In fact, Sarlink and Santoprene are to be considered as dispersions of EPDM rubber in a continuous PP matrix, and the measured diffusion coefficients are a function of the diffusion coefficients of the phases in the dispersion. Investigations into the nature of this function are beyond the scope of the present study.

SANS

The results of the preliminary experiments on Santoprene 281-82 are pointing to the presence of a second phase with a sharp phase boundary, a scattering length very different from the matrix and a domain size > 10 nm. The "objects" with a sharp phase boundary are probably voids. The existence of such voids in polymers is well established.¹⁹ Other phases present are EPDM rubber particles dispersed in the PP matrix and mineral oil. The approximate H/C ratios of those phases are all close to 2, excluding them as potential candidates for the observed scattering. We expected that the size of the voids would be sensitive to change by the extended cyclic loading of the sample. However, little difference can be observed between the $I - Q$ curves of the reference and fatigued samples. The differences between both curves are quasi-nihil, meaning that the void space or distribution of voids over the volume do not change beyond the detection limit of the technique.

Fatigue as imposed in our experiments seems not to influence the SANS of deuterated Sarlink 3280, as far as the distribution of the mineral oil over the different phases of the TPO is concerned (from observation 4). The observed SANS behavior ($\log I - \log Q$ slope around -3) is typical for polymers having a fractal structure and vague boundaries between the phases responsible for SANS contrast.

When Sarlink or Santoprene, having different SANS behavior, are swollen in D₂O + 3% HAC, their behavior becomes very similar ($\log I - \log Q$ slope

-4.2). This could mean that only the contribution of the D₂O to SANS can be observed in our experiments. This contribution is an order of magnitude larger than the contribution of nondeuterated compounds, due to the large scattering length difference between hydrogen ($b = -0.374 \times 10^{-12}$ cm) and deuterium ($b = 0.667 \times 10^{-12}$ cm). During swelling, the D₂O is distributed over the TPO, establishing a rather sharp phase boundary (from observation 1).

Swelling in 3% (v/v) HAC + H₂O does not change the SANS image, although a 3% (v/v) solution of HAC in H₂O causes an equal increase in mass as a 3% (v/v) HAC in D₂O solution. So, the 3% HAC + H₂O solution does, in fact, diffuse into the TPO, but cannot be observed by SANS due to lack of contrast between the TPO and the H₂O. Only the voids in the TPO cause SANS contrast and the distribution of these voids is not altered by the diffusing fluid. The fluid is assumed to fill only the voids and does not alter the distribution or the number of the voids (from observations 2 and 3), but probably only their size (cf. swelling measurements).

Santoprene (sample 6) has a $\log I - \log Q$ slope of -3.9, indicating sharper boundaries between the phases that cause SANS contrast. Sarlink (sample 5) has a $\log I - \log Q$ slope of -3.2, indicating fuzzy boundaries and fractal behavior, since $I(Q) \sim Q^{-(6-f)}$, with f the fractal dimension of the phase boundary.²⁰ For Santoprene, f would be 2.1, and for Sarlink, f would be 2.8. A perfectly smooth phase boundary would result in a dimension of 2. Materials with such phase boundaries are, in principle, more sensitive to fatigue damage because the phase boundaries are crack initiation sites. Based solely on these results, the fatigue resistance of Sarlink 3280 could be deemed superior to that of Santoprene 281-82.

CONCLUSIONS

Under the conditions imposed by our fatigue setup, SANS cannot detect an effect of mechanical fatigue

on the distribution or the size of the voids in Santoprene 281-82 or Sarlink 3280. SANS experiments on fatigued samples with a partly deuterated mineral oil phase did not reveal any influence of fatigue on the distribution of the mineral oil phase over the blend. This means that the load during our fatigue tests was below the endurance limit of the sample materials.

The SANS behavior of control samples Santoprene 281-82 and Sarlink 3280 is, however, quite different. When interpreted in terms of phase boundaries with fractal dimensions, the fractal dimension of the boundary between the phases causing SANS contrast is 2.8 for Sarlink 3280 while it is 2.1 for Santoprene 281-82. This has consequences for the mechanical properties of a material. More fuzzy phase boundaries make a material less prone to crack initiation and fatigue damage.

Absorption of a 3% (v/v) HAC in water solution at 65°C was studied by observing the increase in mass and increase in thickness. The two methods do not yield equivalent results as is apparent from the discrepancies between the calculated diffusion coefficients. However, a significant difference between Sarlink and Santoprene and between fatigued and control samples of each material was observed in the saturation values of liquid uptake. This points for Santoprene 281-82 as compared to Sarlink 3280 to higher porosity or higher pore volume and higher driving force for swelling. However, the influence of fatigue on the calculated diffusion coefficients was not significant.

A grant of IWONL to S.V.J. (910219) is gratefully acknowledged. This research was funded with a specialization scholarship of the Flemish Institute for the Encouragement of Scientific and Technological Research in Industry (IWT). Ing. J. Mariën is acknowledged for his excellent technical assistance with the fatigue experiments.

REFERENCES

1. Y. Kikuchi, T. Fukui, T. Okada, and T. Inoue, *J. Appl. Polym. Sci. Appl. Polym. Symp.*, **50**, 261 (1992).
2. S. Kawabata, S. Kitawaki, H. Arisawa, Y. Yamashita, and X. Guo, *J. Appl. Polymer Sci. Appl. Polym. Symp.*, **50**, 245 (1992).
3. A. Y. Coran, R. P. Patel, and D. Williams, *Rubber Chem. Technol.*, **55**, 116 (1982).
4. T. Tanaka and D. J. Fillmore, *J. Chem. Phys.*, **70**, 1214 (1979).
5. T. Canal and N. A. Peppas, *J. Biomed. Mater. Res.*, **23**, 1183 (1989).
6. P. Chiarelli and D. De Rossi, *Progr. Colloid Polym. Sci.*, **78**, 4 (1988).
7. P. Chiarelli, C. Domenici, and G. Genuini, *J. Mater. Sci. Mater. Med.*, **4**, 5 (1993).
8. P. J. Flory, *Principles of Polymer Chemistry*, Cornell University Press, Ithaca, NY, 1953.
9. J. Bastide and C. Picot, *J. Macromol. Sci.-Phys. B*, **19**, 13 (1981).
10. F. P. Baldwin, *Rubber Chem. Technol.*, **43**, 1040 (1970).
11. G. Kraus, *Rubb. World*, **135**, 67, 254 (1956).
12. J. A. Helsen, S. V. Jaecques, J. Van Humbeeck, and J.-P. Simon, *J. Mater. Sci. Mater. Med.*, **4**, 471 (1993).
13. J. Crank, *The Mathematics of Diffusion*, 2nd ed., Oxford University Press, London, 1979.
14. J. Crank and G. S. Park, in *Diffusion in Polymers*, J. Crank and G. S. Park, Eds., Academic Press, London, 1968, Chap. 1.
15. J. Teixeira, in *Structure and Dynamics of Strongly Interacting Colloids and Supramolecular Aggregates in Solution*, S.-H. Chen et al., Eds., Kluwer, Dordrecht, 1992, Chap. Introduction to Small-angle Neutron Scattering Applied to Colloidal Science, p. 635.
16. J. Teixeira, in *On Growth and Form. Fractal and Non-Fractal Patterns in Physics*, H. E. Stanley and N. Ostrowsky, Eds., Kluwer, Dordrecht, 1986, Chap. Experimental Methods for Studying Fractal Aggregates, p. 145.
17. J. A. Barrie, in *Diffusion in Polymers*, J. Crank and G. S. Park, Eds., Academic Press, London, 1968, Chap. 8.
18. D. Jeschke and H. A. Stuart, *Z. Naturforsch.*, **16a**, 37 (1961).
19. W. O. Statton, *J. Polym. Sci.*, **58**, 205 (1962).
20. H. D. Bale and P. W. Schmidt, *Phys. Rev. Lett.*, **53**, 596 (1984).

Received July 26, 1995

Accepted December 20, 1995